10-13-1995

Mutation or Deletion of the Saccharomyces Cerevisiae RAT3/ NUP133 Gene causes Temperature-Dependent Nuclear Accumulation of Poly(A)+ RNA and Constitutive Clustering of Nuclear Pore Complexes

Ou Li
Dartmouth College

Catherine V. Heath
Dartmouth College

David C. Amberg
Dartmouth College

Thomas C. Dockendorff
Dartmouth College

Connie S. Copeland
Yale University

Molecular Biology of the Cell
Vol. 6, 401–417, April 1995

Mutation or Deletion of the *Saccharomyces cerevisiae RAT3/NUP133* Gene Causes Temperature-dependent Nuclear Accumulation of Poly(A)$^+$ RNA and Constitutive Clustering of Nuclear Pore Complexes

Ou Li,* Catherine V. Heath,* David C. Amberg,*† Thomas C. Dockendorff,* Connie S. Copeland,‡ Michael Snyder,‡ and Charles N. Cole*§

*Department of Biochemistry, Dartmouth Medical School, Hanover, New Hampshire 03755; and ‡Department of Biology, Yale University, New Haven, Connecticut 06511

November 28, 1994; February 17, 1995
Monitoring Editor: Randy W. Schekman

To identify genes whose products play potential roles in the nucleocytoplasmic export of messenger RNA, we isolated temperature-sensitive strains of *Saccharomyces cerevisiae* and examined them by fluorescent in situ hybridization. With the use of a digoxigen-tagged oligo-$(dT)_{50}$ probe, we identified those that showed nuclear accumulation of poly(A)$^+$ RNA when cells were shifted to the nonpermissive temperature. We describe here the properties of yeast strains bearing the *rat3–1* mutation (*RAT* - ribonucleic acid trafficking) and the cloning of the *RAT3* gene. When cultured at the permissive temperature of 23°C, fewer than 10% of cells carrying the *rat3–1* allele showed nuclear accumulation of poly(A)$^+$ RNA, whereas approximately 70% showed nuclear accumulation of poly(A)$^+$ RNA after a shift to 37°C for 4 h. In wild-type cells, nuclear pore complexes (NPCs) are distributed relatively evenly around the nuclear envelope. Both indirect immunofluorescence analysis and electron microscopy of *rat3–1* cells indicated that NPCs were clustered into one or a few regions of the NE in mutant cells. Similar NPC clustering was seen in mutant cells cultured at temperatures between 15°C and 37°C. The *RAT3* gene encodes an 1157-amino acid protein without similarity to other known proteins. It is essential for growth only at 37°C. Cells carrying a disruption of the *RAT3* gene were very similar to cells carrying the original *rat3–1* mutation; they showed temperature-dependent nuclear accumulation of poly(A)$^+$ RNA and exhibited constitutive clustering of NPCs. Epitope tagging of Rat3p demonstrated that it is located at the nuclear periphery and co-localizes with nuclear pore proteins recognized by the RL1 monoclonal antibody. We refer to this nucleoporin as Rat3p/Nup133p.

INTRODUCTION

Export of mRNA from the nuclei of eukaryotic cells is an essential step in gene expression. Fully processed mRNAs exit the nucleus through nuclear pore complexes (NPCs), large complex proteinaceous structures that perforate the double membrane of the nuclear envelope (for reviews, see Gerace, 1992; Hurt, 1993; Newmeyer, 1993; Pante and Aebi, 1993; Rout and Wente, 1994). Large ribonucleoprotein complexes can be visualized in transit through the NPC (Stevens and Swift, 1966; Mehlin *et al.*, 1992) and these same NPCs also serve as channels for nuclear protein import (for reviews, see Silver, 1991; Forbes, 1992).

NPCs are estimated to have a total mass of approximately 125 million daltons (Reichelt *et al.*, 1990), and may contain up to 100 different polypeptides (Snow *et al.*, 1987; Rout and Blobel, 1993; Rout and Wente, 1994). NPCs display eightfold symmetry when exam-

§ Corresponding author.
† Present address: Department of Genetics, Stanford University Medical Center, Stanford, CA 94305.

ined at high resolution in the electron microscope. Three-dimensional image reconstruction suggests that they are comprised of nuclear and cytoplasmic rings, with eight spokes radiating inward toward a central transporter apparatus (Unwin and Milligan, 1982; Akey, 1990, 1991; Reichelt *et al.*, 1990; Jarnik and Aebi, 1991; Hinshaw *et al.*, 1992; Akey and Radermacher, 1993). Under certain preparation conditions, electron microscopy permits filaments to be observed projecting from NPCs into both the nucleoplasm and cytoplasm (Maul, 1977; Richardson *et al.*, 1988; Allen and Douglas, 1989; Jarnik and Aebi, 1991; Ris and Malecki, 1993). The nucleoplasmic filaments sometimes appear organized into basket-like structures, termed the fish-trap (Jarnik and Aebi, 1991; Goldberg and Allen, 1992). NPCs possess 9-nm channels that permit small molecules, including ions and metabolites, to cross the nuclear envelope by passive diffusion. Movement of larger molecules, including proteins and RNAs, is an active process requiring energy and specific signals in the molecules being transported. Recent studies indicate that the small GTP-binding protein Ran/TC4 is one of the factors responsible for protein import in permeabilized vertebrate cells (Melchior *et al.*, 1993; Moore and Blobel, 1993; Ren *et al.*, 1993) and that its yeast homologue, Gsp1p, plays a similar role in *Saccharomyces cerevisiae* (Schlenstedt *et al.*, 1995).

The NPCs of all eukaryotic organisms from yeasts to mammals and plants are believed to be similar in both structure and function (Gerace, 1992; Stewart, 1992; Hurt, 1993; Rout and Wente, 1994). Knowledge of the roles that NPC substructures and specific nucleoporins may have in mRNA export and protein import is limited. Functions for certain nucleoporins have been implied through immunologic, biochemical, and genetic studies. Antibodies against the vertebrate nucleoporin p62 have been shown to inhibit nucleocytoplasmic trafficking of both RNA and proteins in vivo in *Xenopus* oocytes (Dabauvalle *et al.*, 1988; Featherstone *et al.*, 1988). Nup153p from rat liver cells has zinc-finger motifs that have been shown to bind DNA in vitro (Sukegawa and Blobel, 1993). Mutations in several yeast NPC proteins have been reported to result in defects in nucleocytoplasmic transport. Mutants of *NUP49* and *NSP1* have defects in protein import using an in vitro transport assay (Schlenstedt *et al.*, 1993). A conditional allele of *NUP1* has defects in protein import, RNA export, and nuclear structure (Bogerd *et al.*, 1994). A temperature-sensitive RNA export defect was also seen in strains carrying a deletion of the *NUP116* gene. However, in strains with the *NUP116* deletion, the nuclear envelope becomes herniated after a temperature shift, and a seal develops over the NPCs, thus providing a physical barrier to RNA export. Under these conditions, RNA is seen to accumulate in a space external to the nuclear pore but contained within the nuclear envelope seal that forms over the NPCs (Wente and Blobel, 1993). Yeast strains containing a *NUP145* coding region downstream of the *GAL1* promoter and depleted of Nup145p, show nuclear accumulation of poly(A)$^+$ RNA beginning about 3 h after transcription of the *NUP145* gene is blocked by transfer of cells to glucose-containing media; defects in the import of nuclear proteins is seen at later times (Fabre *et al.*, 1994).

To identify cellular components important for mRNA export from the nucleus, we and others developed screens to isolate mutants of *S. cerevisiae* defective in nucleocytoplasmic transport (Amberg *et al.*, 1992; Kadowaki *et al.*, 1992, 1994). Because the NPC plays a central role in mRNA export, we anticipated that this screen would identify mutants with defects in NPC structure and function. We screened a collection of 1200 temperature-sensitive yeast strains by using in situ hybridization to detect cells that had an increased level of poly(A)$^+$ RNA in their nuclei after incubation at the nonpermissive temperature. Genetic analyses have permitted us to focus our studies on those strains for which a single gene defect is responsible for both temperature-sensitive growth and nuclear accumulation of poly(A)$^+$ RNA. We call these *rat* mutants (ribonucleic acid trafficking). We previously described our work on the *RAT1* gene (Amberg *et al.*, 1992). We describe here the *RAT3* gene and the characterization of yeast strains carrying mutations of this gene.

In the course of studying these mutant strains, we examined the subcellular distribution of their NPC proteins by immunofluorescence microscopy using antibodies reactive with NPC Ags. An interesting phenotype was discovered in *rat3* mutant strains. The NPCs were clustered in one or a few regions of the nuclear envelope, rather than being evenly distributed. This NPC clustering was evident in all cells at both permissive and nonpermissive temperatures, whereas defects in mRNA trafficking were detected in few cells at permissive temperature and in most of the cells at nonpermissive temperature. The *RAT3* gene encode a protein of 1157-amino acids that shows no significant similarity to any known proteins. Rat3p is essential for growth only at elevated temperatures (37°C). A null allele generated by disruption of the open reading frame also showed constitutive clustering of NPCs and temperature-conditional nuclear accumulation of poly(A)$^+$ RNA. The results indicate that *RAT3* is important for the proper distribution and function of NPCs. Epitope tagging of the *RAT3* open reading frame permitted the localization of its gene product to NPCs by indirect immunofluorescence. Therefore, Rat3p is a nucleoporin that we refer to as Rat3p/Nup133p.

MATERIALS AND METHODS

Yeast Cell Culture, Strains, Media, Mutant Isolation, and Genetic Methods

The yeast strains used in this work are listed in Table 1 and the plasmids used are listed in Table 2. *S. cerevisiae* were cultured by standard methods (Rose *et al.*, 1989; Sherman, 1991). Wild-type strains FY23 and FY86 were obtained from F. Winston (Harvard Medical School), and were derived from SC288C by making it *GAL2*$^+$ and *ura3–52*. Cells containing mutant alleles of the *RAT3* gene were routinely grown at 23°C on rich (YPD) medium (Sherman, 1991). Standard yeast genetic methods were employed for analysis of phenotypes, strain crosses, dominance/recessive tests, and tetrad dissection.

The isolation of *RAT* mutants has been previously described (Amberg *et al.*, 1992). Briefly a collection of 1200 temperature-sensitive strains generated by mutagenesis with UV light was screened microscopically after in situ hybridization with digoxigenin-tagged oligo-$(dT)_{50}$ to localize poly(A)$^+$ RNA, followed by incubation with fluoresceinated anti-digoxigenin antibodies. Strains exhibiting accumulation of the fluorescent signal in their nuclei were chosen for further study.

For most temperature shift experiments, cells cultured in liquid media at 23°C were shifted to rotating 37°C water or air incubators and incubation was continued as indicated in the figure legends. To determine cell doubling times, single colonies of wild type or mutant yeast cells were inoculated into 5 ml of YPD and allowed to grow for 32 h at 23°C. Cell density was determined with a hemacytometer. Duplicate cultures of each strain were diluted to between 4 and 8 $\times$ 10^6 cells/ml in YPD, recounted, and incubated at 23°C. After 4 h, an aliquot of each culture was removed and counted and one culture from each strain was shifted to 37°C. Duplicate samples were removed from each culture every 4 h and cell concentration was determined by counting. To examine reversion, cells were removed from each culture after 28 h and plated on YPD plates. Plates were incubated at 23°C or 37°C for 1 wk and colony numbers were determined daily.

Cloning and Mapping of the RAT3 Genes

The *RAT3* genes was cloned by complementation of the temperature-sensitive growth defect in strain DAt3–2 (*rat3–1*) by using a genomic library of *S. cerevisiae* DNA (*Sau* 3A partial digestion products) cloned into a *LEU2-CEN* plasmid (F. Spencer and P. Hieter, unpublished observations). This library was transformed into the mutant strain by electroporation and Leu$^+$ colonies were selected at 37°C. Plasmid DNA was isolated from colonies (Rose *et al.*, 1989), transformed into *Escherichia coli*, and plasmids isolated for further analyses. Plasmids were retested for their ability to transform the mutant strain to Leu$^+$ and to grow at 37°C. All the *rat3–1*–complementing plasmids contained overlapping segments of yeast DNA. A blot of electrophoretically separated yeast chromosomes (Clontech Laboratories, Palo Alto, CA) and the filter sets of ordered phage lambda and cosmid clones of the yeast genome (Riles *et al.*, 1993) were probed with a radiolabeled fragment common to all *rat3–1*–complementing clones to determine the chromosomal location of the cloned DNA.

Disruption of the RAT3 Gene

To disrupt the *RAT3* gene, a 6.9-kb *Xba*I-*Nhe*I fragment including the entire *RAT3* gene was excised from plasmid pOL1 and ligated into the polylinker region of pUC19 yielding pOL9. *E. coli* strain GM2163 was transformed with pOL9 to generate unmethylated DNA, which could be digested with *Bcl*I. Then, 92% of the *RAT3* open reading frame (from aa 43 through 1104) was removed by digestion with *Bcl*I and *Nco*I, and a 2.2-kb *Bsp*HI-*Bam*HI fragment, containing the *HIS3* gene was excised from plasmid pRS403 (Sikorski and Hieter, 1989), and inserted into *Nco*I-*Bcl*I–digested pOL9 to yield pOL10. Digestion of pOL10 with *Xba*I and *Afl*II yielded a 6.5-kb fragment containing the complete *HIS3* gene surrounded by the flanking regions of the *RAT3* gene. Viable His$^+$ transformants were selected after integrative transformation (Rothstein, 1991) of the wild-type diploid LGY101 (*his3/his3*) with this fragment. That the fragment had integrated to disrupt one *RAT3* locus in the diploid was confirmed by Southern analysis. This strain, OLY103, was transferred to sporulation media and after several days, tetrads were dissected and allowed to germinate on YPD at 23°C. Cells were then replica plated to SC-HIS plates and plates were incubated at 23°C and 37°C. The strain with the disruption of *RAT3* chosen for further study was designated OLY104.

Table 1. Yeast strains used in this study

Strains	Genotype	Source
Dat3-2	*Mata trp1Δ63 leu2Δ1 ura3-52 rat3-1*	This study
Dat3xt3	*Mata/Matα ura3-52/ura3-52 leu2Δ1/leu2Δ1 trp1Δ63/TRP1 his3 Δ200/HIS3 rat3-1/rat3-1*	This study
OLY101	*Matα his3Δ200 leu2Δ1 ura3-52 rat3-1*	This study
FY23	*Mata trp1Δ63 leu2Δ1 ura3-52*	Provided by F. Winston
FY86	*Matα his3Δ200 leu2Δ1 ura3-52*	Provided by F. Winston
FY23×86	*Mata/Matα ura3-52/ura3-52 leu2Δ1/leu2Δ1 trp1Δ63/TRP1 his3 Δ200/HIS3*	This study
OLY102	*Mata trp1Δ63 leu2Δ1 ura3-52 RAT3::URA3*$^+$*RAT3*	This study
LGY101	*Mata/Matα his3Δ200/his3 Δ200 leu2Δ1/leu2Δ1 ura3-52/ura3-52*	L. Gorsch
OLY103	*Mata/Matα his3Δ200/his3Δ200 leu2Δ1/leu2Δ1 ura3-52/ura3-52 RAT3/RAT3::HIS3*	This study
OLY104	*Mata his3Δ200 leu2Δ1 ura3-52 RAT3::HIS3*	This study
OLY106	*Mata trp1Δ63 leu2Δ1 ura3-52 rat3-1 pOL11(LEU2 RAT3*$_{myc}$*)*	This study
OLY107	*Mata his3Δ200 leu2Δ1 ura3-52 RAT3::HIS3 pOL11(LEU2 RAT3*$_{myc}$*)*	This study
LDY97	*Matα leu2-3,112, ura3-52 his3 NUP1::LEU2 (CEN HIS3* plasmid bearing *nup1-106* allele)	Provided by L. Davis

Table 2. Plasmids used in this study

Plasmids	Markers	Comments	Source
Yeast/bacterial shuttle plasmids			
pOL1	*CEN4 LEU2*	putative *RAT3* clone No.1 in p366	This study
pOL2	*CEN4 LEU2*	putative *RAT3* clone No.2. in p366	This study
pOL4	*CEN4 URA3*	geneA^a in YCplac33	This study
pOL5	*CEN4 URA3*	gene B^a (*RAT3*) in YCplac33	This study
pOL6	*CEN4 URA3*	genes C^a and D^a in YCplac33	This study
pOL7	*CEN4 URA3*	gene E^a in YCplac33	This study
pOL8	*URA3*	gene B^a (*RAT3*) in YIplac211	This study
pOL11	*CEN4 LEU2*	myc epitope-tagged *RAT3* in pOL2	This study
Bacterial plasmids			
pOL3		0.8Kb XbaI-ClaI fragment of pOL1 in $pBlueSK^+$	This study
pOL9		6.8Kb XbaI-NheI fragment including *RAT3* in pUC19	This study
pOL10		disruption of *RAT3* by *HIS3* in pOL9	This study

[a]These letters correspond to the open reading frames shown in Figure 4A.

Integration of an Auxotrophic Marker Adjacent to RAT3

A 4.6-kb *Xba*I-*Kpn*I fragment from pOL1, containing part of the *RAT3* gene, was ligated into the polylinker region of YIPlac211 (Gietz and Sugino, 1988), which had been digested with *Xba*I and *Kpn*I, to create pOL8. The plasmid was linearized within the *RAT3* sequences by digestion with *Spe*I, and transformed into wild-type strain FY23. Cells were grown on SC-URA plates for 4 days. Colonies were selected and the pattern of integration of the *RAT3*-YIPlac211 sequences determined by Southern analysis. A strain, OLY102, with the correct pattern for integration at the *RAT3* locus was mated to OLY101 (carrying the *rat3–1* mutation), and diploids were grown in sporulation media for 7–14 days. Tetrads were dissected and the genotypes of haploids tested.

In Situ Hybridization and Indirect Immunofluorescence

The procedure for in situ hybridization has been described (Amberg *et al.*, 1992). The probe used to detect poly(A)$^+$ RNA was oligo(dT)$_{50}$ to which 1–4 digoxigenin-dUTP molecules were added at the 3′ end by using terminal deoxynucleotidtyl transferase. DAPI (4′, 6-diamidino-2-phenylindole-dihydrochloride), a DNA-binding dye, was used to localize the nuclear region of cells. Previous studies have demonstrated that the fluorescein isothiocyanate-tagged (FITC) anti-digoxigenin signal is specific for poly(A)$^+$ RNA and dependent on active transcription by RNA polymerase II (Amberg *et al.*, 1992).

Immunofluorescence on fixed yeast cells using anti-Rat7p/Nup159p antibody (Gorsch *et al.*, 1995) or antibody RL1 (Snow *et al.*, 1987) was performed as previously described (Mirzayan *et al.*, 1992; Copeland and Snyder, 1993). RL1 is a mouse monoclonal IgM that recognizes multiple nuclear pore proteins in both mammalian cells and in yeast, and was generously provided by Dr. Larry Gerace (Scripps Research Institute, La Jolla, CA). Secondary donkey anti-mouse antibodies tagged with CY3 or FITC were obtained from Jackson Immunoresearch (West Grove, PA). The anti-Rat7p/Nup159p antibody was raised in guinea pigs to a GST-fusion protein containing most of the repeat region of the yeast nucleoporin Rat7p/Nup159p (Gorsch *et al.*, 1995) and as a secondary antibody, FITC-conjugated goat anti-guinea pig IgG (Vector Labs, Burlingame, CA). This antibody recognizes a single polypeptide on Western blots that has been shown to be the *RAT7/NUP159* gene product (Gorsch *et al.*, 1995) and shows a punctate rim staining pattern that is co-extensive with the RL1 staining pattern. FITC-conjugated goat anti-guinea pig IgG was used as a secondary antibody (Vector Labs).

Indirect immunofluorescence was also performed to detect the subcellular distribution of a fusion protein consisting of the first 33 amino acids of yeast histone H2B (containing its nuclear localization signal) fused to *E. coli* β-galactosidase, and under the control of a modified *GAL1* promoter (Moreland *et al.*, 1987). Strains were transformed with pP_{GAL}H2B-NLS-LacZ, the plasmid encoding this reporter protein. Stationary phase cultures of yeast cells were diluted 1:50 and grown overnight at 23°C in SC-ura medium containing 2% raffinose. The next morning, aliquots of each culture were shifted to 36°C for 2.5 h and then galactose was added to all cultures to a final concentration of 2%. Incubation was continued an additional 1.5 h before cells were fixed. Indirect immunofluorescence was performed using a mouse monoclonal antibody to *E. coli* β-galactosidase (Sigma Chemical, St. Louis, MO) diluted 1:2000. The secondary antibody, FITC-conjugated horse anti-mouse IgG (Vector Labs), was used at a 1:650 dilution.

Electron Microscopy

Electron microscopy was performed by a modification of published procedures (Byers and Goetsch, 1991). Cells were cultured at 23°C in YPD to a density of 0.2–2 × 10^7cells/ml. Cells were harvested by filtration, and were fixed for 2 h at room temperature in 3% (vol/vol) glutaraldehyde containing 0.1% tannic acid in 0.1 M sodium cacodylate, pH 6.8. Fixed cells were washed twice in 50 mM KH_2PO_4/K_2HPO_4, pH 7.5, and then digested with 125 mg/ml Zymolyase 100T (Seikagaku, Rockville, MD) in 50 mM KH_2PO_4/K_2HPO_4, pH 7.5, for 40 min at 30°C. After two washes in 0.1 M sodium cacodylate, pH 6.8, the spheroplasted cells were treated with 2% (wt/vol) OsO_4 in 0.1 M sodium cacodylate, pH 6.8, for 1 h on ice. Samples were washed and stored overnight at 4°C in 0.1 M sodium cacodylate, pH 6.8. Samples were next washed three times in ddH_2O and treated for 1 h with 2% uranyl acetate in ddH_2O. After two washes in ddH_20, cells were embedded in 2% agar, dehydrated through graded ethanol, and embedded in Spurr's medium. Thin sections were cut, stained with uranyl acetate and Reynold's lead citrate, and examined on a JEOL 100CX electron microscope at 60 kV accelerating voltage.

Epitope Tagging and Immunolocalization

The DNA encoding three copies of the epitope recognized by the 9E10 anti-myc monoclonal antibody (EQKLISEEDLN) was isolated by PCR using as primers 5′ATTGGATATGGACTAGTCAAGATC-

TCGTACGCATTCGAGCTCGGTACCCGGGGATCC and 5'GCGGGATTGGACTAGTAAGATCTCGTACGCAAGCTTGCATGCCTGCAGGTCGAC and as a template plasmid pKK-1 (obtained from G. Fink, Whitehead Institute, Cambridge, MA). This plasmid is a derivative of pUC119 and contains a triplication of the epitope recognized by the 9E10 monoclonal antibody. Primers were obtained from Bio-Synthesis, Inc. (Lewisville, TX). These primers introduce *Bsi*WI sites at each end of the PCR amplification product. The PCR product was digested with *Bsi*WI and inserted into the only *Bsi*WI site in the *RAT3* gene (see Figure 4 below; the inserted epitope is at amino acid 895). This leads to the insertion of the following amino acid sequence at this site: FELGTRGSSRGEQKLISEEDLNGEQKLISEEDLNGEQKLISEEDLNGSSRVDLQACKL. The three repeats of the recognized epitope are underlined.

The resulting plasmid (pOL11) was transformed into strain Dat3–2 carrying the *rat3–1* mutation, yielding strain OLY106, and into strain OLY104, carrying the disruption of *RAT3*, yielding strain OLY107. Cells were grown to early log phase and fixed with 1/10 vol of 37% formaldehyde for 1 h. Cells were then washed three times with 1.2 M sorbitol/50 mM K_2HPO_4, pH 7.5 (solution A), resuspended into 1 ml of solution A with 30 mg of 100T Zymolyase and incubated at room temperature for 10–60 min until spheroplasts were formed. Spheroplasts were washed once with solution A and adhered to polylysine-coated 12-well slides. Samples were washed sequentially with phosphate buffered-saline + 0.1% bovine serum albumin (solution B), solution B + 0.1% NP-40, and solution B, with a 5-min incubation per wash. Cells were incubated with the 9E10 mouse IgG monoclonal anti-myc antibody (a gift from Dr. J.M. Bishop, University of California, San Francisco, CA) in solution B overnight at 4°C. Cells were then washed with solution B, solution B + 0.1% NP-40, and solution B, each for 5 min. Cells were incubated with secondary antibody, FITC-conjugated goat anti-mouse IgG in solution B for 2 h at room temperature, and then washed with solution B, solution B + 0.1% NP-40 and containing 10 μg of DAPI per ml, and solution B, each for 5 min. Cells were mounted with mounting solution, 70% glycerol in phosphate buffered-saline and containing 1 mg *p*-phenylenediamine per ml.

To examine the localization of Rat3p, cells were doubly stained with both the 9E10 anti-"myc" epitope monoclonal antibody and the RL1 anti-nucleoporin monoclonal antibody. The anti-myc antibody is an IgG whereas the RL1 antibody is an IgM. Horse secondary antibodies coupled to FITC and specific for IgG and coupled to Texas Red and specific for IgM (both from Vector Labs) were used at a 1:500 dilution. Control experiments indicated that there was no detectable signal in the Texas Red channel when both primary antibodies and the FITC-conjugated secondary antibody were used; similarly, there was no detectable signal in the FITC channel when both primary antibodies and only the Texas Red-conjugated secondary antibody were used.

RESULTS

Mutation of the RAT3 Gene Causes Nuclear Accumulation of Poly(A)$^+$ RNA at the Nonpermissive Temperature but Does Not Affect Nuclear Protein Import

Figure 1 shows the distribution of poly(A)$^+$ RNA in wild-type and *rat3–1* mutant cells. In wild-type cells either incubated at 23°C (Figure 1A) or shifted to 37°C for 4 h (Figure 1C), the fluorescent signal was relatively uniform throughout the cell. Figure 1, B and D, shows simultaneous DAPI fluorescence and visible light images of the same fields of cells shown in Figure 1, A and C, respectively. At the permissive temperature (23°C), 10% or fewer of *rat3–1* cells showed accumulation of poly(A)$^+$ RNA in their nuclei (Figure 1E) but within 4 h after a shift to 37°C, this percentage rose to about 70% (Figure 1G). Figure 1, F and H, shows combined DAPI fluorescence and visible light images of the same fields of cells shown in Figure 1, E and G, respectively. One cell at the edge of the field in Figure 1G shows two spots of RNA staining; this was a relatively common phenotype of *rat3–1* mutant cells (our unpublished results). *rat3–1* mutant cells shifted to 37°C for 8 or 12 h did not show an appreciable increase in penetrance of the nuclear poly(A)$^+$ RNA accumulation phenotype compared with cells that had been shifted for 4 h (our unpublished results). We showed previously (Amberg *et al.*, 1992) that in situ hybridization with this digoxigenin-tagged oligo-dT_{50} probe detects poly(A)$^+$ RNA. The data in Figure 1 indicate that mutation of the *RAT3* gene results in nuclear accumulation of poly(A)$^+$ RNA upon a shift to the nonpermissive temperature. Diploid cells homozygous for the *rat3–1* mutation showed an essentially identical pattern of accumulation of poly(A)$^+$ RNA after a shift to 37°C (our unpublished results).

To determine whether cells carrying the *rat3–1* mutation also had defects in nuclear protein import, we used indirect immunofluorescence to examine the subcellular distribution of a fusion protein consisting of the nuclear localization signal (NLS) of the yeast histone H2B gene fused to *E. coli* β-galactosidase (Moreland *et al.*, 1987), and expressed from the *GAL1* promoter. As a positive control, we used cells carrying the *nup1–106* allele, which is known to have a defect in nuclear protein import (Bogerd *et al.*, 1994). Dilute cultures were grown overnight at 23°C and were in early log phase the next morning. Aliquots were either maintained at 23°C or shifted to 36°C. We used 36°C as a nonpermissive temperature because the *GAL1* promoter is induced considerably more efficiently at 36°C than at 37°C (L.C. Gorsch and C.N. Cole, unpublished results). After 2.5 additional hours of incubation, transcription of the reporter gene was induced by addition of galactose to all cultures to a final concentration of 2%. Incubation was continued an additional 1.5 h before cells were fixed and processed for indirect immunofluorescence.

In *rat3–1* cells grown continuously at 23°C (Figure 2K) or shifted to 36°C for 4 h (Figure 2M), the fusion protein was detected exclusively in the nucleus. Production of the fusion protein was limited to the last 90 min of the 4 h incubation at 36°C. The fusion protein was also detected entirely in nuclei in wild-type cells, either grown continuously at 23°C (Figure 2A) or shifted to 36°C for 4 h (Figure 2C). In *nup1–106* cells, fusion protein was located primarily in nuclei in the culture maintained at 23°C (Figure 2F), but there was a dramatic accumulation of the reporter protein in the cytoplasmic compartment in *nup1–106* cells shifted to 36°C for 4 h (Figure 2H). Although the *rat3–1* mutation

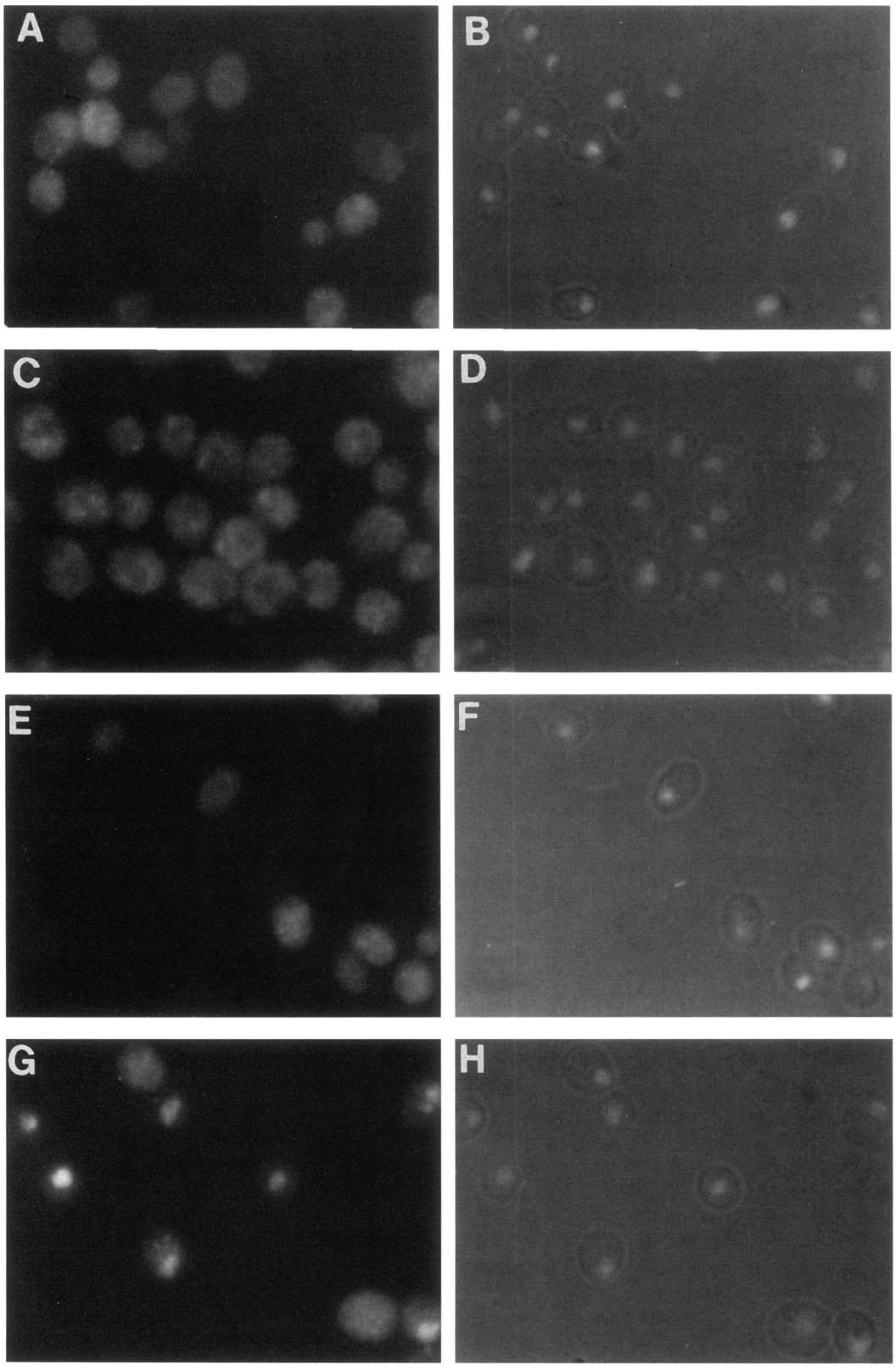

Figure 1. Poly(A)$^+$ RNA accumulates in the nuclei of *rat3–1* mutant cells. Wild-type (FY23) and *rat3–1* cells (strain Dat3–2) were grown to early log phase in YPD at 23°C. Aliquots either held at 23°C or shifted to 37°C for 4 h were fixed and analyzed by in situ hybridization with a digoxigenin-tagged oligo(dT)$_{50}$ probe. Panels A, C, E, and G show the FITC signal, which indicates the location of poly(A)$^+$ RNA. Panels B, D, F, and H show DAPI staining of the same fields of cells as panels A, C, E, and F, respectively. (A and B) Wild-type incubated at 23°C; (C and D) wild-type cells shifted to 37°C for 4 h; (E and F) *rat3–1* cells incubated at 23°C; (G and H) *rat3–1* cells shifted to 37°C for 4 h.

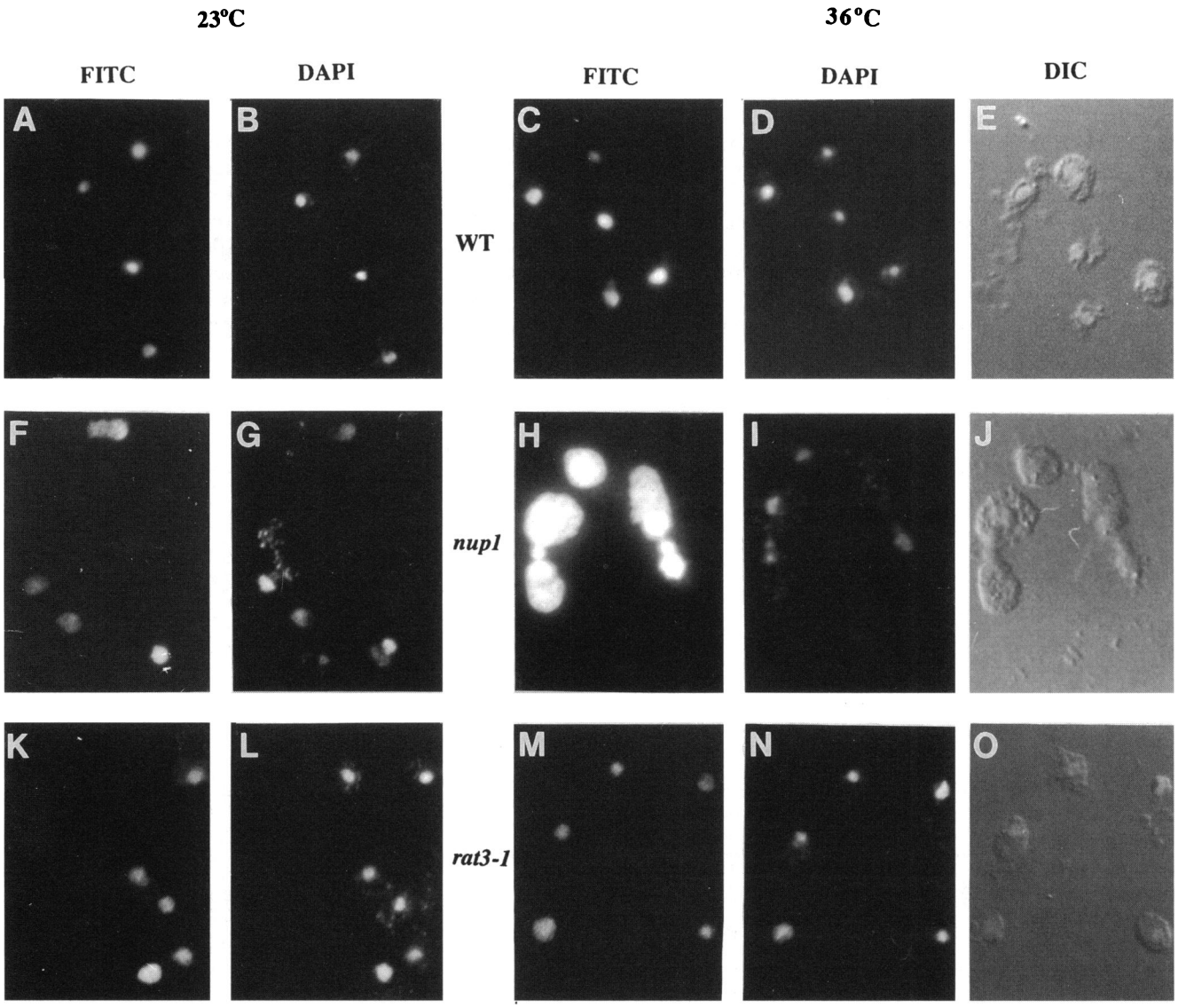

Figure 2. Nuclear protein import occurs normally in *rat3–1* mutant cells. Wild-type (FY86) (panels A-E), *nup1–106* (panels F-J), and *rat3–1* (panels K-O) cells were either incubated continuously at 23°C (A, B, F, G, K, and L) or shifted to 36°C (C, D, E, H, I, J, M, N, and O) for 2.5 h before addition of galactose to induce expression of the reporter protein consisting of the histone H2B nuclear localization signal fused to *E. coli* β-galactosidase. Galactose was added and was continued an additional 90 min before cells were fixed and processed for indirect immunofluorescence. (A) WT, 23°C, FITC; (B) same field of cells as in panel A, stained with DAPI; (C) WT, 36°C, FITC; (D) same field of cells as in panel C, stained with DAPI; (E) same field of cells as in panel C, viewed by DIC microscopy; (F) *nup1–106*, 23°C, FITC; (G) same field of cells as in panel F, stained with DAPI; (H) *nup1–106*, 36°C, FITC; (I) same field of cells as in panel H, stained with DAPI; (J) same field of cells as in panel I, viewed by DIC microscopy; (K) *rat3–1*, 23°C, FITC; (L) same field of cells as in panel K, stained with DAPI; (M) *rat3–1*, 36°C, FITC; (N) same field of cells as in panel M, stained with DAPI; (O) same field of cells as in panel M, viewed by DIC microscopy.

has a dramatic effect on export of poly(A)$^+$ RNA at the nonpermissive temperature, there was no detectable effect of the mutation on nuclear protein import.

Genetic and Physiologic Analyses of the rat3 Mutation

Backcrosses of a haploid *rat3–1* strain with a wild-type strain, followed by subsequent sporulation of resulting diploids and analysis of over 40 tetrads, showed that the temperature-sensitive growth observed in the *rat3–1* strain segregated in a 2:2 ratio and was therefore most likely due to a single gene defect. Seven tetrads, including four from a third backcross, were examined for co-segregation of temperature sensitivity and the defective RNA export phenotype. In all seven cases, the two phenotypes

co-segregated with a 2:2 ratio. Analysis of heterozygous diploids indicated that the phenotypes of temperature-sensitivity and nuclear poly(A)$^+$ RNA accumulation were both recessive.

Cells carrying the *rat3–1* mutation were tested for their growth characteristics (Figure 3A). The wild-type culture had a doubling time at 23°C of approximately 2 h. At 23°C, the mutant strain grew more slowly with a doubling time of approximately 3 h. After the shift to 37°C, the growth rate of the wild-type strain was unaltered but it grew to a slightly lower final density at 37°C than at 23°C. After the shift to 37°C, the *rat3–1* mutant strain continued to grow at approximately the same rate at 37°C as it had at 23°C for the next 8 h, after which its doubling time increased dramatically to approximately 12–14 h and the culture reached a final cell concentration substantially below that obtained by continuous growth at 23°C. Revertants did not accumulate during incubation of *rat3–1* mutant cells at 37°C; after 28 h at that temperature, approximately 12% of the cells retained viability.

No specific cell cycle arrest phenotype was seen when *rat3–1* mutant cells were cultured for 4 h at 37°C; furthermore, when *rat3–1* cells were synchronized by treatment with α-factor and then released into the cell cycle, the kinetics with which cells displayed nuclear

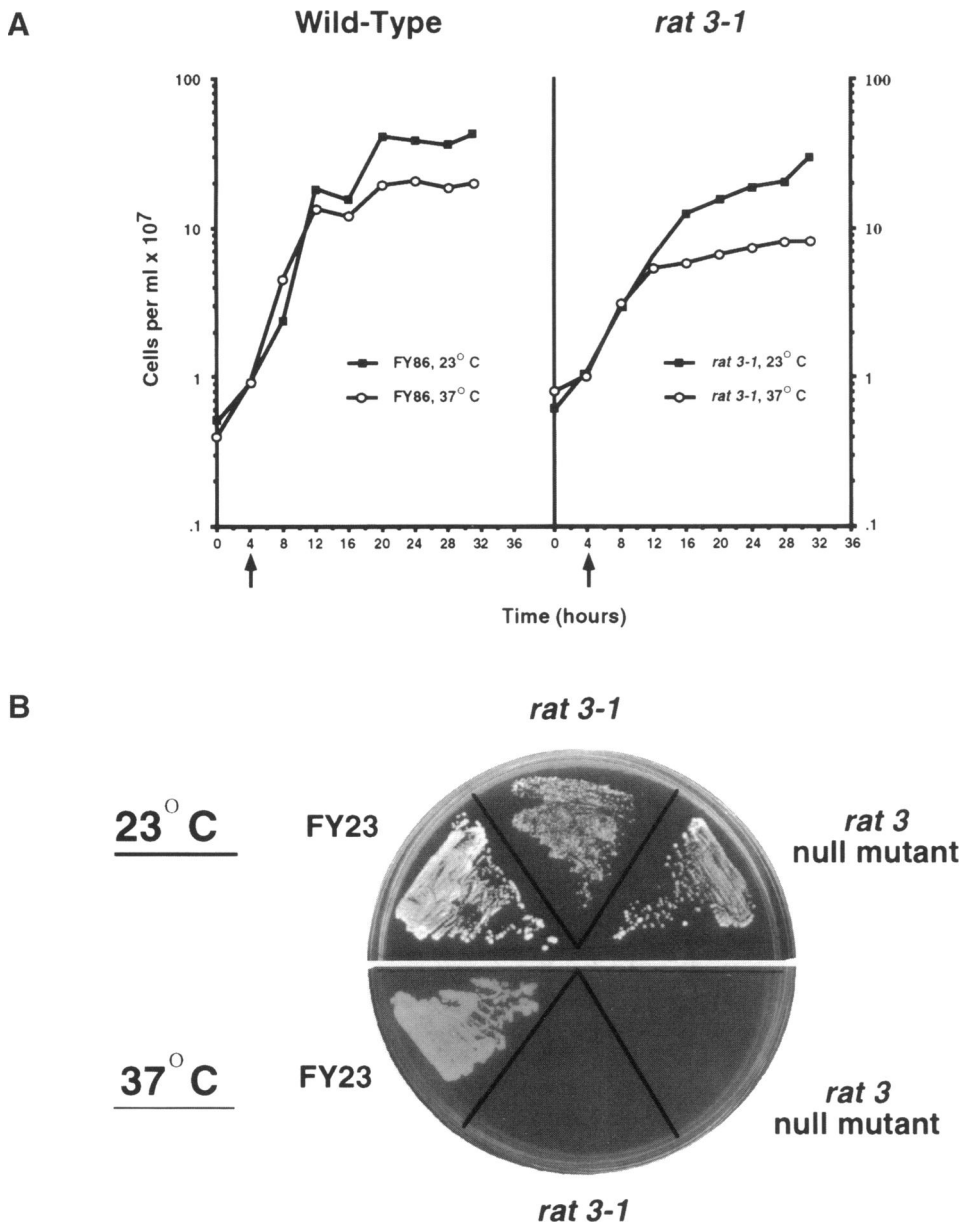

Figure 3. Growth properties of yeast cells carrying the *rat3–1* mutation. (A) Growth curves of wild-type (FY23) and *rat3–1* mutant cells (Dat3–2). Cells were grown at 23°C to early log phase. At the point indicated in the figure, aliquots of each strain were shifted to 37°C. Cell density was determined by using a hemacytometer to count cells. (B) The *RAT3* gene is not essential for growth at 23°C, but is essential at 37°C. Wild-type cells (FY23), *rat3–1* cells, and cells with a disruption of *RAT3* were grown on YPD plates at either 23°C or 37°C. The plates were photographed after 3 days of growth.

accumulation of poly(A)$^+$ RNA was the same as for unsynchronized cells (our unpublished results). These observations suggest that the phenotypes seen are unrelated to the cell cycle.

Cloning and Mapping of RAT3

The temperature sensitivity caused by the *rat3–1* mutation was used to clone the *RAT3* gene by complementation using a *CEN* library. Several complementing plasmids were analyzed by restriction endonuclease digestion. All complementing plasmids yielded related digestion patterns with multiple restriction endonucleases. A restriction map of the complementing clone with the smallest yeast DNA insert is shown in Figure 4A. A 1.5-kb *Bsm*I fragment of this clone was used to physically map the cloned DNA. Hybridization to a chromosome blot indicated that the putative *RAT3* clone is located on Chr. XI. This same *Bsm*I fragment identified a single cosmid clone derived from the region of Chr. XI containing the *PRP16* gene. A small portion of one end of the complementing DNA was se-

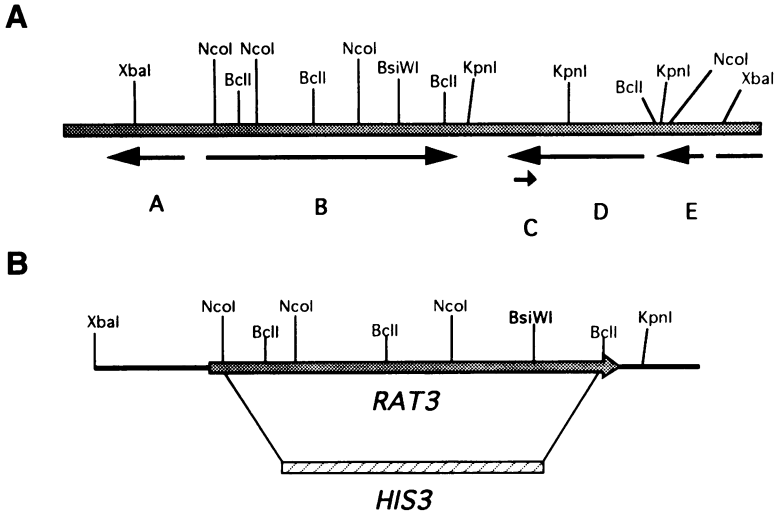

C

```
MSEKKVHLRL RKELSVPIAV VENESLAQLS YEEESQASLM DISMEQQQLR  50
LHSHFDNSKV FTENNRYIVK TLQTDYSSGF SNDDELNGYI DMQIGYGLVN 100
DHKKVYIWNI HSTQKDTPYI TVPFRSDDND EIAVAPRCIL TFPATMDESP 150
LALNPNDQDE TGGLIIIKGS KAIYYEDINS INNLNFKLSE KFSHELELPI 200
NSSGGEKCDL MLNCEPAGIV LSTNMGRIFF ITIRNSMGKP QLKLGKLLNK 250
PFKLGIWSKI FNTNSSVVSL RNGPILGKGT RLVYIITTNKG IFQTWQLSAT 300
NSHPTKLIDV NIYEAILESL QDLYPFAHGT LKIWDSHPLQ DESSQLFLSS 350
IYDSSCNETY YILSTIIFDS SSNSFTIFST YRLNTFMESI TDTKFKPKIF 400
IPQMENANDT NEVTSILVMF PNAVVITQVN SKLDSSYSMR RKWEDIVSLR 450
NDIDIIGSGY DSKSLYVLTK QMGVLQFFVK ENEETNSKPE VGFVKSHVDQ 500
AVYFSKINAN PIDFNLPPEI SLDQESIEHD LKLTSEEIFH SNGKYIPPML 550
NTLGQHLSVR KEFFQNFLTF VAKNFNYKIS PELKLDLIEK FEILNCCIKF 600
NSIIRQSDVL NDIWEKTLSN YNLTQNEHLT TKTVVINSPD VFPVIFKQFL 650
NHVVFVLFPS QNQNFKLNVT NLINLCFYDG ILEEGEKTIR YELLELDPME 700
VDTSKLPWFI NFDYLNCINQ CFFDFTFACE EEGSLDSYKE GLLKIVKILY 750
YQFNQFKIWI NTQPVKSVNA NDNFININNL YDDNHLDWNH VLCKVNLKEQ 800
CIQIAEFYKD LSGLVQTLQT LDQNDSTTVS LYETFFNEFP KEFSFTLFEY 850
LIKHKKLNDL IFRFPQQHDV LIQFFQESAP KYGHVAWIQQ ILDGSYADAM 900
NTLKNITVDD SKKGESLSEC ELHLNVAKLS SLLVEKDNLD INTLRKIQYN 950
LDTIDAEKNI SNKLKKGEVQ ICKRFKNGSI REVFNILVEE LKSTTVVNLS 1000
DLVELYSMLD DEESLFIPLR LLSVDGNLLN FEVKKFLNAL VWRRIVLLNA 1050
SNEGDKLLQH IVKRVFDEEL PKNNDFPLPS VDLLCDKSLL TPEYISETYG 1100
RFPIDQNAIR EEIYEEISQV ETLNSDNSLE IKLHSTIGSV AKEKNYTINY 1150
ETNTVEY*
```

Figure 4. The *RAT3* gene. (A) Schematic representation of the yeast DNA common to plasmid members of the *CEN* library that complemented the *rat3–1* mutation. Key restriction endonuclease sites are shown. The arrows show the five complete putative ORFs (A through E) in this region. The partial ORF of *PRP16* is at the far right side. ORF B proved to be *RAT3*. (B) The *RAT3* gene and the strategy for disruption of*RAT3*. The *RAT3* ORF is shown by the thick arrow. Ninety-two percent of the *RAT3* ORF (from amino acids 43–1104) was deleted by digestion with *Nco*I and *Bcl*I, followed by insertion of a DNA fragment containing the *HIS3* gene. The *Bsi*WI site, which was used to insert three copies of myc-epitope for *Rat3p* immunolocalization, is also shown. (C) The predicted 1157-amino acid sequence of Rat3p.

quenced and found to contain sequences encoding part of the open reading frame of *PRP16*. Using this information, we obtained DNA sequence extending in both directions from the *PRP16* gene. Restriction endonuclease digestion patterns permitted a determination of which portion of the DNA sequence provided corresponded to the complementing library clone. Within this region were five open reading frames (Figure 4A). Subclones of each (A through E) were prepared in YCplac33 (Gietz and Sugino, 1988), and a subclone containing a 4.6-kb *Xba*I-*Kpn*I fragment (plasmid pOL5) was able to complement both the temperature sensitivity and RNA export defect of strains carrying the *rat3–1* mutation. No portion of the *PRP16* gene is contained in this complementing region. The open reading frame included in this fragment encodes a protein of 1157 amino acids (Figure 4C) and is designated YKR082w in the published sequence of yeast chromosome XI (Dujon *et al.*, 1994; Garcia-Cantalejo *et al.*, 1994). We refer to this gene as *RAT3/NUP133* because it encodes a nucleoporin (see below). This same gene has been identified independently by Doye *et al.* (1994).

To show that the cloned fragment in pOL1 and pOL5 likely contained the wild-type form of the *rat3–1* mutant gene rather than a suppressor of it, the *URA3* gene and complementing DNA from pOL1 were integrated into the genome of wild-type FY23 at the site of the putative *RAT3* gene via homologous recombination. This strain was mated with the *rat3–1* mutant strain, and subsequent tetrad analysis showed that the *URA3* marker segregated away from the temperature-sensitive *rat3–1* allele in 65 of 67 haploid progeny strains. This strongly suggests that the cloned DNA from pOL1 complements the *rat3–1* defects and is not acting as a suppressor.

One copy of the *RAT3* gene was disrupted in a diploid strain by replacing 92% of the coding region (from amino acid 43 through 1104) with the *HIS3* gene (Figure 4B). This strain was sporulated, and tetrads were dissected. Most of the tetrads (85%) yielded four viable spores. All four-spore tetrads contained two His^+ and two His^- spores, indicating that the *RAT3* gene is not essential. Cells carrying a disruption of *RAT3* were temperature sensitive for growth and accumulated poly(A)$^+$ RNA in their nuclei after a shift to 37°C (our unpublished results). The disruption strain appeared phenotypically very similar to the original strain carrying the *rat3–1* allele but a higher percentage of cells showed nuclear accumulation of poly(A)$^+$ RNA at both 23°C (approximately 40% compared with 10% for strains carrying the *rat3–1* mutation) and 37°C (100% compared with approximately 70% for *rat3–1* strains). Thus, the *RAT3* gene is essential for growth only at elevated temperatures (Figure 3B).

NPC Ags Are Mislocalized in Yeast Strains Containing Mutations within the RAT3 Gene

The NPC plays a critical role in nucleocytoplasmic transport. Because the NPC contains more than 100 different polypeptides, it is likely that some mutants identified in our screen will have defects in the structure, function, or assembly of NPCs. Therefore, we performed immunofluorescence analysis on yeast cells bearing the *rat3–1* allele using an antibody raised in guineas pigs to a GST-fusion protein containing part of the repeat-containing nucleoporin Rat7p/Nup159p. This antibody recognizes a single band on Western blots of yeast extracts, and this band has been shown to be the product of the *RAT7/NUP159* gene (Gorsch *et al.*, 1995).

Immunofluorescence micrographs of wild-type yeast and the *rat3–1* strain are shown in Figure 5. Anti-Rat7p/Nup159p (anti-NPC) antibody binding sites were visualized by using a second antibody coupled to FITC and nuclei of cells were localized by staining with DAPI. In wild-type cells (Figure 5A), anti-Rat7p/Nup159p antibody stained the nuclear periphery in a discontinuous or punctate manner, a pattern indicative of NPC staining. A weak cytoplasmic signal was also seen. The nuclear rim staining completely surrounds the DAPI-stained DNA region (Figure 5B). When *rat3–1* cells were stained with anti-Rat7p/Nup159 antibody, a very different pattern was seen. Instead of discontinuous staining around the nuclear rim, the NPC Ags were clustered in an area adjacent to rather than surrounding the DNA region (Figure 5, C and D). In these *rat3–1* cells, the anti-Rat7p/Nup159p Ags were grouped into one or two smaller patches. All of the cells examined (more than 200) exhibited this clustering phenotype. Essentially identical results were obtained when indirect immunofluorescence was performed on *rat3–1* cells using the RL1 antibody, which has previously been shown to recognize NPC epitopes from cells of vertebrates and yeast (Snow *et al.*, 1987; Copeland and Snyder, 1993). Clustering of NPC Ags was unchanged in the *rat3–1* mutant strain and the *HIS3*-disrupted strain after a shift to a nonpermissive temperature for up to 4 h (our unpublished results). Genetic analyses showed that the NPC clustering is recessive, and cosegregated with temperature sensitivity and nuclear accumulation of poly(A)$^+$ RNA, indicating that NPC clustering is another manifestation of these *rat3* alleles.

Unlike the mislocalization of pore complex Ags in *rat3* cells, which was observed at permissive as well as restrictive temperatures, accumulation of mRNA in the nucleus was dependent upon the incubation temperature. Nuclear RNA accumulation occurred in a large majority of cells at the elevated temperature, but only in a small subpopulation at permissive temperature. We investigated whether the difference in tem-

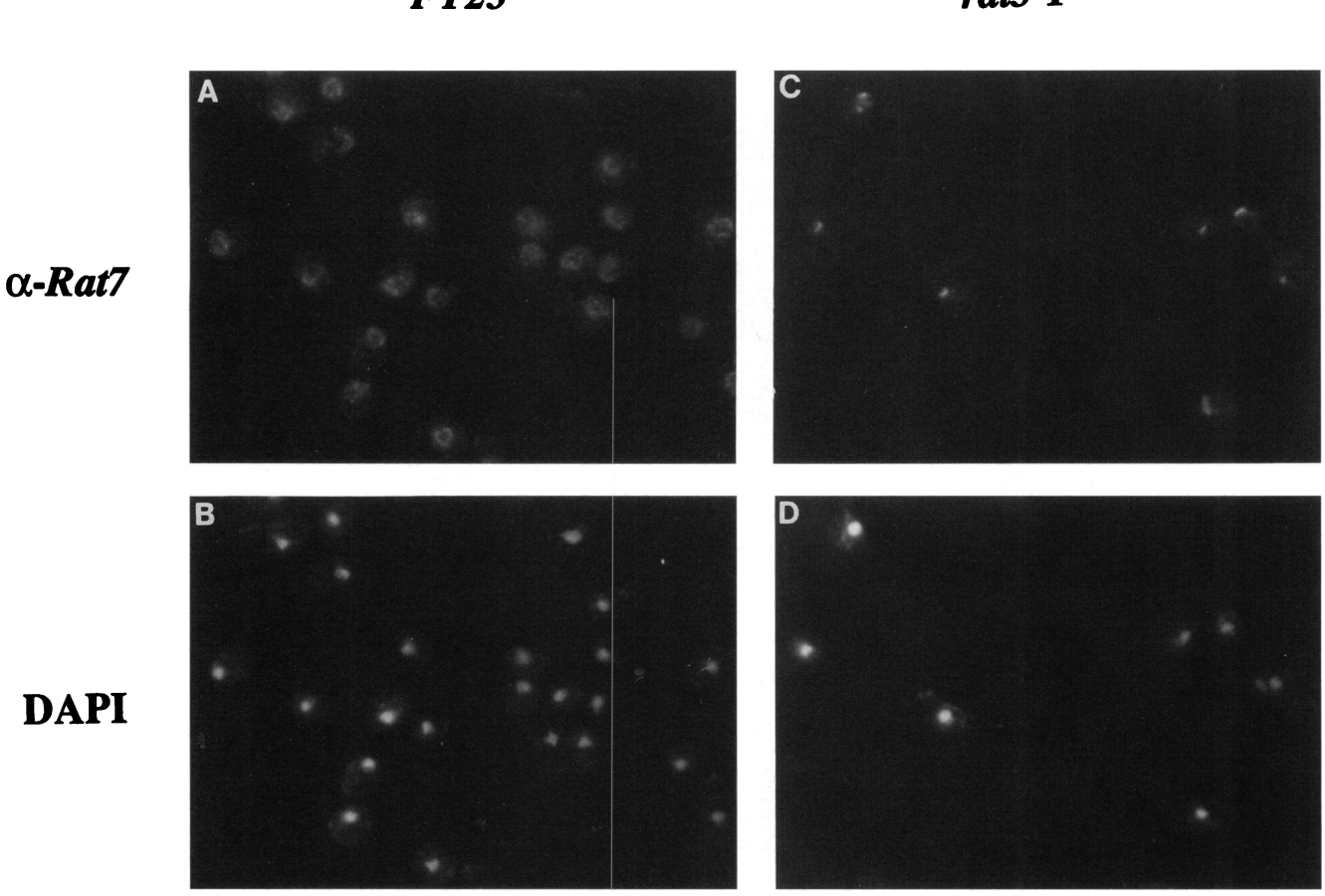

Figure 5. Immunofluorescence microscopy indicates that NPC Ags are mislocalized in *rat3–1* cells. FY23 (wild-type) cells and *rat3–1* cells (Dat3–2) were grown at 23°C, fixed and processed for indirect immunofluorescence microscopy with anti-nuclear pore antibody (anti-Rat7p/Nup159p; Gorsch *et al.*, 1995) reactive with the yeast nucleoporin Rat7p/Nup159p (panels A and C). B and D show DAPI staining of the same fields of cells shown in panels A and C, respectively. A and B: FY23. In wild-type cells, NPC Ags are distributed around the nuclear envelope. C and D: *rat3–1*. NPC Ags in *rat3–1* are clustered in one or two regions of the nuclear envelope.

perature induction of the two phenotypes resulted from a lower threshold temperature for pore complex Ag mislocalization than for mRNA accumulation. To examine this possibility, indirect immunofluorescence using anti-Rat7p/Nup159p antibody was performed on cells cultured at 15°C. Clustering of the pore complex Ags was also observed in the *rat3–1* strain cultured continuously at 15°C. Thus, the *rat3–1* mutation caused conditional retention of mRNA in the nucleus at nonpermissive temperature (37°C) and constitutive mislocalization of NPC Ags at all temperatures tested.

Electron Microscopy Indicates that NPCs Are Clustered in rat3–1 Mutant Cells

The clustering of anti-Rat7p/Nup159p Ags in mutant cells could reflect either a mislocalization of specific pore complex proteins or a mislocalization of whole NPCs. To address this question, we examined the position of NPCs in diploid wild-type and mutant cells by electron microscopy. Figure 6 shows the results of an experiment using diploid cells incubated at 23°C. For wild-type cells, NPCs were distributed around the nuclear envelope (Figure 6A), although occasional local concentrations were observed, as has been previously reported (Severs *et al.*, 1976). In contrast, in diploid cells homozygous for the *rat3–1* mutation, NPCs were observed primarily in one or two discrete areas of the nuclear envelope. Most of the remainder of the nuclear envelope was usually barren of pore complexes, though occasional isolated NPCs were sometimes seen (see Figure 6B). No gross differences were observed in the morphology of the nucleoplasm or the

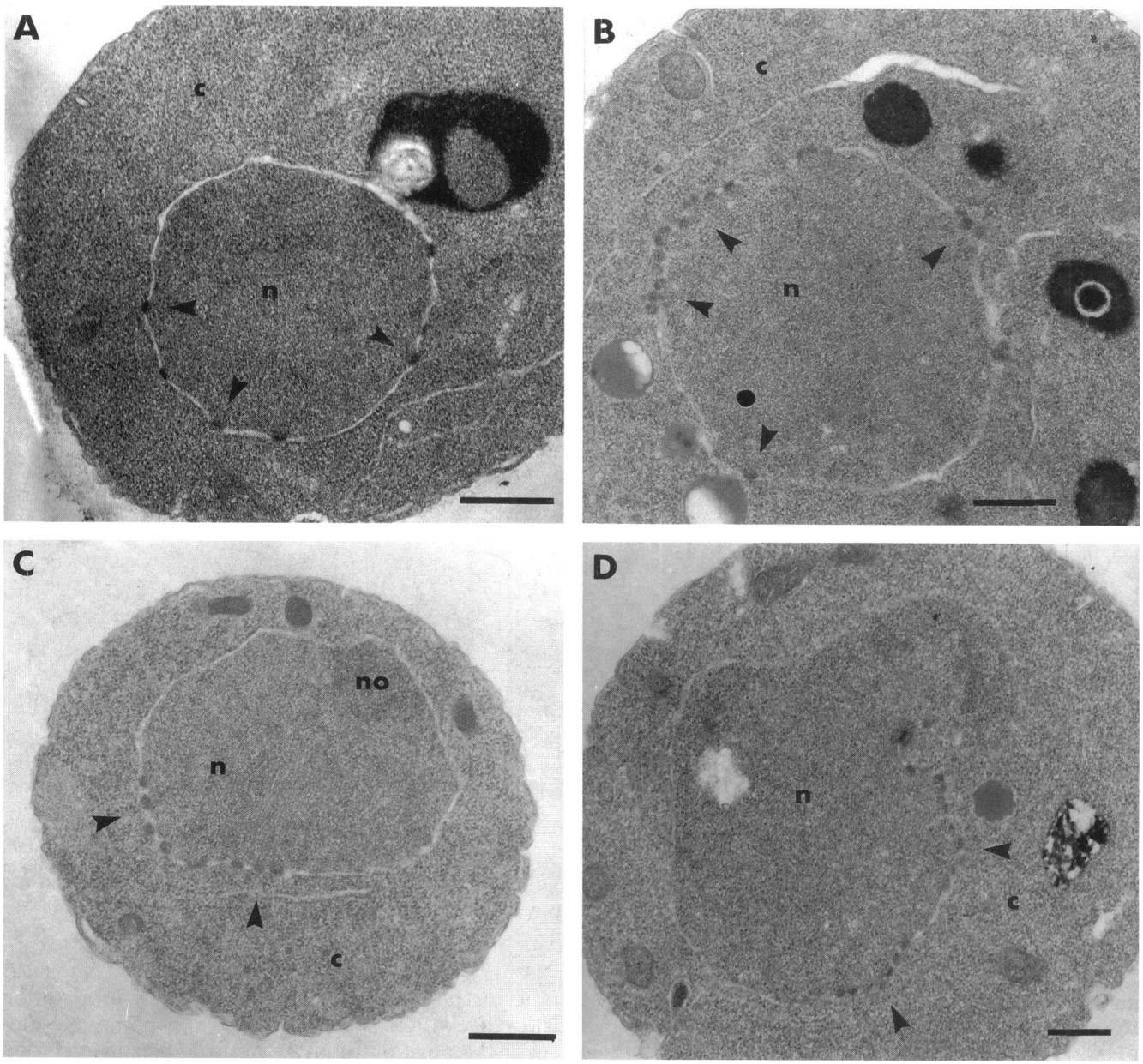

Figure 6. Electron microscopy confirms that NPCs are clustered in *rat3–1* mutant cells. Thin-section electron micrographs of wild-type (FY23X86) and *rat3–1* cells (Dat3xt3) incubated at 23°C. NPCs, recognized as dark bars at interruptions in the NE, are distributed around the NE in wild-type cells and are clustered in *rat3–1* cells. Arrowheads point toward NPCs. (A) Wild-type; (B-D) *rat3–1* cells. n - nucleus; c - cytoplasm; no - nucleolus. Bars, 0.5 μM in each panel.

nucleolus in cells carrying mutant alleles of *RAT3*, as compared with wild-type cells. A small segment of the nucleolus (no) is visible in Figure 6C.

The results from electron microscopy extend the immunofluorescence observations and demonstrate clearly that whole NPCs were clustered in the plane of the nuclear envelope. Thus pore complexes apparently underwent assembly and insertion into the nuclear membrane in cells carrying the *rat3–1* mutation, but failed to be distributed properly around the nuclear periphery. At this low level of resolution, the pore complexes appear to have normal morphology. Electron microscopy analysis of serial sections of *rat3–1* cells indicated that mutant cells contained approximately the same number of NPCs as normal cells and that large regions of the mutant cell nuclear envelope were devoid of NPCs (Copeland, unpublished results).

Immunolocalization of Rat3p

We examined the subcellular location of the protein encoded by the *RAT3* gene. To epitope tag this protein, three copies of the myc epitope recognized by monoclonal antibody 9E10 were inserted into the *RAT3* gene carried on a plasmid. The epitope-tagged *RAT3* construct (epitope located adjacent to amino acid 895 at the *Bsi*WI site; see Figure 4B) was able to complement the temperature sensitivity, nuclear poly(A)$^+$ RNA accumulation, and nuclear pore–clustering defects of cells carrying the *rat3–1* mutation or carrying a disruption of *RAT3*. To localize Rat3p, we performed indirect immunofluorescence on a strain carrying a null allele of the *RAT3* gene and harboring the plasmid encoding the epitope-tagged *RAT3* construct. A punctate staining pattern at the nuclear rim was seen when these cells were stained with the 9E10 anti-myc monoclonal antibody (Figure 7A). Figure 7B shows that an identical punctate pattern was seen when the same field of cells was reacted with the anti-nucleoporin RL1 antibody (Figure 7B). Figure 7C shows the DAPI-stained image of the same field of cells shown in Figure 7, A and B. The co-localization of staining with both anti-myc–epitope and RL1 antibodies indicates that Rat3p is a nucleoporin. In a separate double-staining experiment, co-localization of immunofluorescence was also seen when the 9E10 anti-myc monoclonal antibody and the polyclonal anti-Rat7p/Nup159p antibody were employed (our unpublished results). Therefore, Rat3p is a nucleoporin which we designate as Rat3p/Nup133p.

DISCUSSION

The RAT3/NUP133 Gene and Protein

In this report we describe the cloning and characterization of a new yeast gene, *RAT3*, which is predicted to encode a 133-kDa protein. When epitope tagged, Rat3p was localized to the nuclear rim in a pattern identical to that of the Ags recognized by the anti-nucleoporin antibody RL1. A similar punctate nuclear rim staining pattern has been seen for all yeast NPC proteins whose localization has been examined (Davis and Fink, 1990; Nehrbass *et al.*, 1990; Wimmer *et al.*, 1992; Yano *et al.*, 1992; Loeb *et al.*, 1993; Fabre *et al.*, 1994; Wente and Blobel, 1994; Wozniak *et al.*, 1994) and has only been seen for nuclear pore proteins. Combinations of mutant alleles of nucleoporins are often lethal (synthetic lethality) (Wimmer *et al.*, 1992; Loeb *et al.*, 1993; Belanger *et al.*, 1994; Wente and Blobel, 1994). The *rat3–1* allele shows synthetic lethality with a mu-

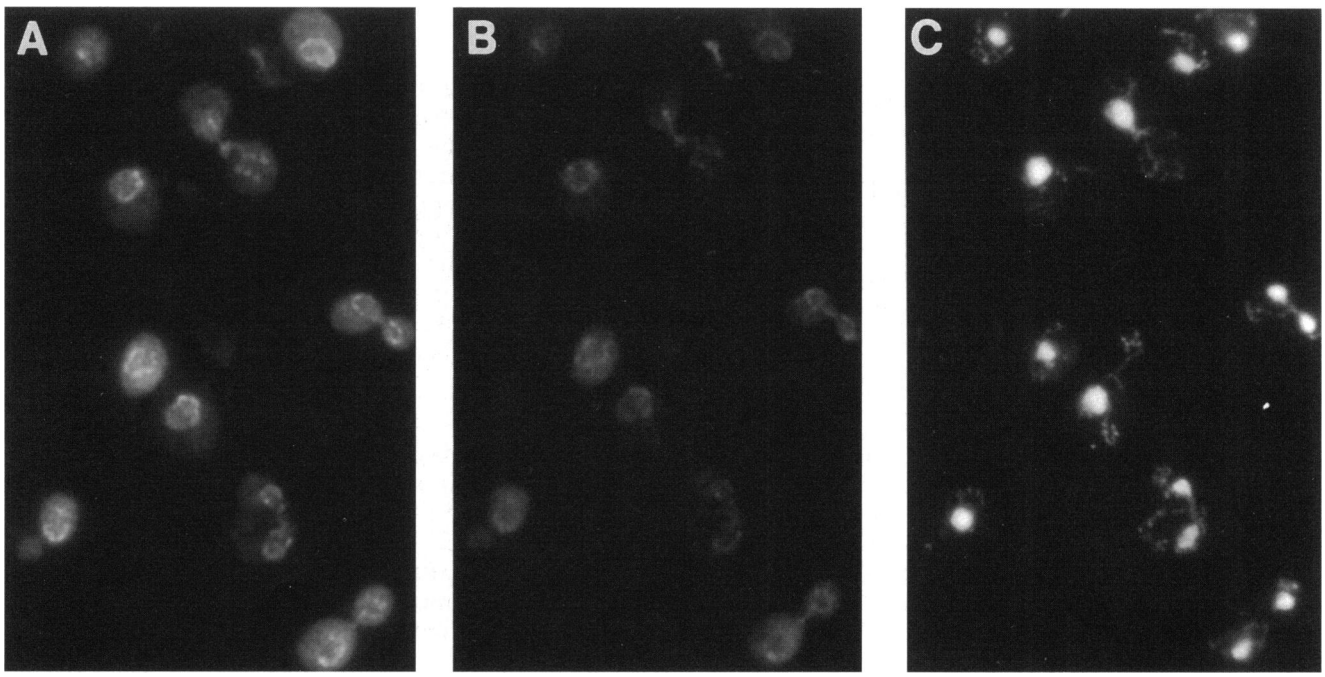

Figure 7. Immunolocalization of Rat3p. Cells carrying a disruption of *RAT3* were transformed with a plasmid (pOL11) that encodes an myc epitope-tagged Rat3p, yielding strain OLY107. Cells were grown to early log phase, fixed, and processed for indirect immunofluorescence microscopy. (A) Indirect immunofluorescence with anti-myc monoclonal antibody 9E10 and an FITC-conjugated secondary antibody. (B) The same field of cells as seen in panel A, stained with the RL1 anti-nucleoporin monoclonal antibody and a Texas Red-conjugated secondary antibody. (C) DAPI staining of the same field of cells as in panels A and B.

tant allele of *RAT7/NUP159*, a repeat-containing NPC protein (Gorsch *et al.*, 1995; Gorsch, Heath, and Cole, unpublished data). On these bases, we conclude that Rat3p is a nuclear pore protein, and we call it Rat3p/Nup133p. The *RAT3/NUP133* gene has also been identified in a synthetic lethal screen for genes whose products interact with Nup49 (Doye *et al.*, 1994).

Mutant cells carrying either the originally isolated *rat3–1* allele or a disruption of *RAT3/NUP133* shared the following phenotypes: 1) Temperature-dependent accumulation of poly(A)$^+$ RNA in nuclei. The percentage of cells, however, showing nuclear accumulation of poly(A)$^+$ RNA was higher at both 23°C and 37°C in the strain carrying a disruption of *RAT3* than in the strain carrying the original *rat3–1* allele. Although only 10% of *rat3–1* cells showed nuclear RNA accumulation at 23°C, the percentage of cells with a *rat3* disruption showing this phenotype at 23°C was about 40%. After a shift to 37°C, the percentage of cells showing this phenotype increased to 70% for *rat3–1* cells and to 100% for cells with a disruption of *rat3*. This suggests that the protein encoded by the *rat3–1* allele retains partial function. 2) Constitutive clustering of NPCs. This phenotype was seen in all cells examined by immunofluorescence for both the *rat3–1* allele and for cells with a disruption of *RAT3*. Defects in nuclear envelope morphology, nucleolar integrity, or in any other aspects of nuclear structure were not noted during examination of the *rat3–1* mutant strain by electron microscopy. *RAT3/NUP133* is essential only at elevated temperatures.

To date, several nuclear pore proteins from *S. cerevisiae* have been described [for review, see (Rout and Wente, 1994)]. Most of these nucleoporins are characterized by the presence of unique repeat motifs that are present in 12–30 copies. Nup1p (Davis and Fink, 1990), Nup2p (Loeb *et al.*, 1993), and Nsp1p (Nehrbass *et al.*, 1990) are members of the XFXFG-repeat–containing family. A second group of yeast nucleoporins that includes Nup49p, Nup100p, Nup116p (Wente *et al.*, 1992; Wimmer *et al.*, 1992; Wente and Blobel, 1994), and Nup145p (Fabre *et al.*, 1994; Wente and Blobel, 1994) have repeats of GLFG in their N-terminal and central domains. Nic96p (Grandi *et al.*, 1993), a major component of the yeast NPC by mass (Rout and Wente, 1994), lacks repeats, whereas Srp1p contains eight degenerate repeats that are related to repeats seen in plakoglobin, β-catenin, and the *Drosophila* armadillo protein (Yano *et al.*, 1992, 1994). A tenth yeast protein, POM152p, is thought to be a membrane protein (Wozniak *et al.*, 1994), is not essential, and is also a very abundant component of the yeast NPC (Rout and Blobel, 1993). Because the NPC is thought to have up to 100 different polypeptides, many more remain to be described. The *RAT3/NUP133* protein is novel in that it lacks any significant similarity with any known proteins. Rat3p/Nup133p is an acidic protein with a calculated pI of 4.82. Our analyses do not permit us to determine whether Rat3p/Nup133p forms part of the basic framework structure of the NPC or is a peripheral component, or whether it is located at the cytoplasmic face, the nucleoplasmic face, or both.

Nuclear Accumulation of Poly(A)$^+$ RNA

The *rat3–1* mutant was first identified by a fluorescent in situ hybridization screen to identify yeast mutants with altered patterns of localization of poly(A)$^+$ RNA. We previously used this screen to identify and characterize the *RAT1* gene (Amberg *et al.*, 1992), and several additional mutants are currently being characterized. We anticipated that some mutants identified would affect intranuclear movement of mRNA and pre-mRNA whereas others would affect NPCs, because these are the structures through which all classes of RNA exit the nucleus.

In the *rat3–1* mutant, the nuclear accumulation of poly(A)$^+$ RNA appeared in about 70% of the cells after a shift to a nonpermissive temperature and was seen at permissive temperature in a small percentage of *rat3–1* cells in any given population. One explanation for the partial penetrance of RNA export defects is a model that invokes a threshold of export activity below which a dramatic failure in export results. Catastrophic defects in export could result from failure to export the mRNA for the *RAT3/NUP133* gene itself at restrictive temperature or perhaps the mRNAs encoding other proteins required for mRNA export. Small differences between cells in a population could result in cells reaching this threshold at different times after a shift to nonpermissive temperature. At permissive temperature, the function of the mutant Rat3p/Nup133p protein or an NPC lacking Rat3p/Nup133p is most likely partially compromised, resulting in slowed export or partial nuclear accumulation of mRNA in certain cells. *rat3/nup133* mutant cells appear to have a partially compromised mRNA export apparatus at permissive temperature, leading some cells to cross this threshold.

NPC Defects

During our screen for mutants in RNA export, we expected to find among our mutant collection mutations linked to NPC function. Unexpectedly, mutation of *RAT3/NUP133* (either the original *rat3–1* allele or the null allele) affected NPCs by altering their distribution in the nuclear envelope. At both permissive and restrictive temperatures, nuclear pores were clustered in one or two regions of the nuclear envelope, and large areas of the nuclear envelope were devoid of pores. Accumulation of RNA at nonpermissive temperature is suggestive of a block in transport through the NPC, but could also result from a failure of the transport substrate (hnRNP) to associate with the

NPC. At the relatively low resolution of our transmission electron microscopy experiments, the NPCs of *rat3–1* cells have apparently normal structure. Furthermore, immunoblotting with anti-NPC antibodies indicated no major change in the level of the NSP1 protein in *rat3–1* cells grown at room temperature or 37°C (C.S. Copeland and F. McKeon, unpublished results). Future studies can address with greater biochemical and morphological resolution the composition and structure of the pore complexes in the mutant cells. At our present level of understanding, however, the NPCs of *rat3–1* cells appear to be properly assembled and inserted into the nuclear envelope. Furthermore, they apparently function well enough at permissive temperature to support near wild-type rates of growth. We do not know at this time how clustered pores might be divided between mother and daughter cells at mitosis. An unequal distribution between mother and daughter cells may well account for the differences observed in growth rates between wild-type and *rat3–1* cells.

Whether or not NPCs are normal in these mutants, mutation or deletion of the *RAT3/NUP133* gene clearly alters the distribution of NPCs in the nuclear envelope. NPCs are usually evenly distributed around the nucleus in most somatic cell types [reviewed by (Maul, 1977)], including yeast, although the distribution may not be perfectly random (Severs *et al.*, 1976). Several specialized cell types have highly ordered NPC arrangements. Apparent rearrangement of NPCs into clusters is seen during the differentiation of spermatocytes to spermatozoa in several species, so that the area of the nuclear envelope underlying the acrosome is devoid of pore complexes (Maul, 1977). Thus, the dramatic NPC mislocalization seen in the *rat3–1* mutant is not without precedent, and could represent a distortion of a normal process.

Mutation of other yeast NPC proteins has also been associated with defects in NPC distribution or interactions with the nuclear envelope. Yeast cells carrying a deletion of the *NUP116* gene are temperature sensitive for growth (Wente *et al.*, 1992; Wimmer *et al.*, 1992). Such strains display NPC-studded invaginations of the inner nuclear membrane at the permissive temperature, and at the nonpermissive temperature they acquire membrane herniations and seals form over these NPCs (Wente and Blobel, 1993). At the nonpermissive temperature, these seals form a barrier to mRNA export. Deletion of the amino-terminal half of the *NUP145* gene results in clustering of NPCs (Wente and Blobel, 1994). When examined in the electron microscope, the NPCs in cells bearing this partial deletion of *NUP145* display localized "grapelike" clusters of NPCs interconnected by a network of nuclear envelope herniations (Wente and Blobel, 1994). The clustering defects seen in cells bearing mutations of *RAT3/NUP133* are distinct from defects associated with deletion of *NUP116* or partial deletion of *NUP145*. In contrast to cells with a deletion of *NUP116*, no intranuclear annulate lamellae were seen in *rat3–1* mutant cells. No large-scale herniation of the nuclear envelope was seen, although at the level of resolution seen in Figure 6, it is not possible to say that there are no abnormalities of the nuclear envelope.

We can envision several mechanisms that might lead to the NPC-clustering defect. Distinguishing between these options may help elucidate the normal process of NPC biogenesis. For example, NPCs could be inserted into the nuclear envelope at a defined site and remain at this location in the *rat3–1* mutant. Thus the defect would affect a mechanism to distribute the pore complexes around the nuclear periphery. This hypothesis implies that at some stage in their biogenesis pore complexes are mobile in the yeast nuclear envelope. In an alternative hypothesis, NPC insertion could occur around the nuclear envelope but the NPCs would not be anchored in the mutant cells and could redistribute into clusters. The distribution of NPCs within the nuclear envelope would thus be dependent on anchoring to the nucleoskeleton, the cytoskeleton, or both. The *rat3–1* mutant could be defective in anchoring pore complexes to these skeletal structures. We think it is unlikely that NPC clusters in *RAT3/NUP133* mutants reflect aggregation of mutant pore complexes because of physical/chemical interactions between the mutant NPCs. In electron micrographs of mutant cells showing NPC clusters, each pore within a cluster sometimes appeared to be surrounded by a portion of the nuclear envelope (Figure 6C), suggesting that NPCs do not necessarily make direct contact with one another when clustered. In addition, the examination of isolated nuclei indicates that once formed, the NPC clusters do not redistribute in the absence of gross connections to the cytoskeleton (Copeland and Snyder, unpublished results). Thus the presence of NPC clusters does not depend on the continuous presence of an intact cytoskeleton. Little is currently known about how NPCs are assembled or inserted or how they become distributed throughout the nuclear envelope; however, proper NPC distribution may affect the efficiency of nuclear export.

The most surprising aspect of the NPC clustering seen in mutant cells is the fact that these cells grow and export mRNA almost normally at the permissive temperature of 23°C, despite displaying the pore complex–clustering defect at all temperatures examined. In this respect, it is relevant that a small fraction of cells in any population does accumulate RNA in the nucleus even at permissive temperature. The increased severity of the RNA accumulation phenotype at 37°C could be explained in several ways. The *RAT3/NUP133* gene could perform multiple functions, one in NPC localization in the nuclear envelope, and an additional function, required only at elevated temper-

atures, related to mRNA export. Alternatively, processes important for RNA export that are specified by other genes may be temperature sensitive in the absence of functional Rat3pNup133p.

ACKNOWLEDGMENTS

We thank Dr. Larry Gerace for providing antibody RL1, J. Michael Bishop for a gift of monoclonal antibody 9E10, B. Dujon and A. Jimenez for providing DNA sequence information for *S. cerevisiae* chromosome XI before its publication, and Drs. Joel Rosenbaum and Dan Finley for use of equipment. We thank Drs. Beth Jones, Fred Winston, and Laura Davis for providing strains. We thank J. Loeb for providing a plasmid. C.S.C. thanks Barry Piekos for advice and assistance with electron microscopy and Dr. Frank McKeon for providing laboratory space for a portion of this work. We are also grateful to Lisa Gorsch and the other members of the Cole laboratory for interesting discussions and technical advice. We also thank Valerie Doye and Eduard Hurt for sharing with us their findings about *NUP133*. This work was supported by grants from the National Institutes of Health, Public Health Service (GM-33998 to C.N.C. and GM-36494 to M.S.) and by a Pew Scholar award to M.S. C.S.C. was supported in part by the Department of Radiation Oncology, University of Massachusetts Medical Center, and by a Charles A. King Trust Fellowship from the Medical Foundation.

REFERENCES

Akey, C.W. (1990). Visualization of transport-related configurations of the nuclear pore transporter. Biophys. J. *58*, 341–355.

Akey, C.W. (1991). Probing the structure and function of the nuclear pore complex. Semin. Cell Biol. *2*, 167–177.

Akey, C.W., and Radermacher, M. (1993). Architecture of the *Xenopus* nuclear pore complex revealed by three-dimensional cryo-electron microscopy. J. Cell Biol. *122*, 1–19.

Allen, J.L., and Douglas, M.G. (1989). Organization of the nuclear pore complex in *Saccharomyces cerevisiae*. J. Ultrastruct. Mol. Struct. Res. *102*, 95–108.

Amberg, D.A., Goldstein, A.L., and Cole, C.N. (1992). Isolation and characterization of *RAT1*: an essential gene of *Saccharomyces cerevisiae* required for the efficient nucleocytoplasmic trafficking of mRNA. Genes Dev. *6*, 1173–1189.

Belanger, K.D., Kenna, M.A., Wie, S., and Davis, L.I. (1994). Genetic and physical interactions between Srp1p and nuclear pore complex proteins Nup1p and Nup2p. J. Cell Biol. *126*, 619–630.

Bogerd, A.M., Hoffman, J.A., Amberg, D.C., Fink, G.R., and Davis, L.I. (1994). *nup1* mutants exhibit pleiotropic defects in nuclear pore complex function. J. Cell Biol. *127*, 319–332.

Byers, B., and Goetsch, L. (1991). Preparation of yeast cells for thin-section electron microscopy. Methods Enzymol. *194*, 602–608.

Copeland, C.S., and Snyder, M. (1993). Nuclear pore complex antigens delineate nuclear envelope dynamics in vegetative and conjugating *Saccharomyces cerevisiae*. Yeast *9*, 235–249.

Dabauvalle, M.-C., Loos, K., Merkert, H., and Scheer, U. (1988). Monoclonal antibodies to a M_r 68,000 pore complex glycoprotein interfere with nuclear protein uptake in *Xenopus* oocytes. Chromosoma *97*, 193–197.

Davis, L.I., and Fink, G.R. (1990). The NUP1 gene encodes an essential component of the yeast nuclear pore complex. Cell *61*, 965–978.

Doye, V., Wepf, R., and Hurt, E.C. (1994). A novel nuclear pore protein Nup133p with distinct roles in poly(A)$^+$ RNA transport and nuclear pore distribution. EMBO J. *13*, 6062–6075.

Dujon, B., Alexandraki, D., Andre, B., Ansorge, W., Baladron, V., (1994). Complete DNA sequence of yeast chromosome XI. Nature *369*, 371–378.

Fabre, E., Boelens, W.C., Wimmer, C., Mattaj, I.W., and Hurt, E.C. (1994). Nup145p is required for nuclear export of mRNA and binds homopolymeric RNA in vitro via a novel conserved motif. Cell *78*, 275–289.

Featherstone, C., Darby, M.K., and Gerace, L. (1988). A monoclonal antibody against the nuclear pore complex inhibits nucleocytoplasmic transport of protein and RNA in vivo. J. Cell Biol. *107*, 1289–1297.

Forbes, D.J. (1992). Structure and function of the nuclear pore complex. Annu. Rev. Cell Biol. *8*, 495–527.

Garcia-Cantalejo, J., Baladron, V., Esteban, P.F., Santos, M.A., Bou, G., Remacha, M.A., Revuelta, J.L., Ballesta, J.P., Jimenez, A., and del Rey, F. (1994). The complete sequence of an 18,002 bp segment of *Saccharomyces cerevisiae* chromosome XI contains the *HBS1*, *MRP-L20* and *PRP16* genes, and six new open reading frames. Yeast *10*, 231–245.

Gerace, L. (1992). Molecular trafficking across the nuclear pore complex. Curr. Opin. Cell Biol. *4*, 637–645.

Gietz, R.D., and Sugino, A. (1988). New yeast-*Escherichia coli* shuttle vectors constructed with in vitro mutagenized yeast genes lacking six-base pair restriction sites. Gene *74*, 527–534.

Goldberg, M.W., and Allen, T.D. (1992). High resolution scanning electron microscopy of the nuclear envelope: the baskets of the nucleoplasmic face of the nuclear pores. J. Cell Biol. *119*, 1429–1440.

Gorsch, L.C., Dockendorff, T.C., and Cole, C.N. (1995). A conditional allele of the novel repeat-containing yeast nucleoporin Rat 7 / NUP159 causes both rapid cessation of mRNA export and reversible clustering of nuclear pore complexes. J. Cell Biol. *129*, (*in press*).

Grandi, P., Doye, V., and Hurt, E.C. (1993). Purification of NSP1 reveals complex formation with "GLFG" nucleoporins and a novel nuclear pore protein NIC96. EMBO J. *12*, 3061–3071.

Hinshaw, J.E., Carragher, B.O., and Milligan, R.A. (1992). Architecture and design of the nuclear pore complex. Cell *69*, 1133–1141.

Hurt, E.C. 1993. The nuclear pore complex. FEBS Lett. *325*, 76–80.

Jarnik, M., and Aebi, U. (1991). Toward a more complete 3-D structure of the nuclear pore complex. J. Struct. Biol. *107*, 291–308.

Kadowaki, T., Chen, S., Hitomi, M., Jacobs, E., Kumagai, C., Liang, S., Schneiter, R., Singleton, D., Wisniewska, J., and Tartakoff, A.M. (1994). Isolation and characterization of *Saccharomyces cerevisiae* mRNA transport-defective (mtr) mutants. J. Cell Biol. *126*, 649–659.

Kadowaki, T., Zhao, Y., and Tartakoff, A.M. (1992). A conditional yeast mutant deficient in mRNA transport from nucleus to cytoplasm. Proc. Nat. Acad. Sci. USA *89*, 2312–2316.

Loeb, J., Davis, L.I., and Fink, G.R. (1993). NUP2, a novel yeast nucleoporin, has functional overlap with other proteins of the nuclear pore complex. Mol. Biol. Cell *4*, 209–222.

Maul, G.G. (1977). The nuclear and cytoplasmic pore complex: structure, dynamics, distribution and evolution. Int. Rev. Cytol. Suppl. *6*, 75–186.

Mehlin, H., Daneholt, B., and Skoglund, U. (1992). Translocation of a specific premessenger ribonucleoprotein particle through the nuclear pore studied with electron microscope tomography. Cell *69*, 605–613.

Melchior, F., Paschal, B., Evans, J., and Gerace, L. (1993). Inhibition of nuclear protein import by nonhydrolyzable analogues of GTP

and identification of the small GTPase Ran/TC4 as an essential transport factor. J. Cell Biol. *123*, 1649–1659.

Mirzayan, C., Copeland, C.S., and Snyder, M. (1992). The *NUF1* gene encodes an essential coiled-coil related protein that is a potential component of the yeast nucleoskeleton. J. Cell Biol. *116*, 1319–1332.

Moore, M.S., and Blobel, G. (1993). The GTP-binding protein Ran/TC4 is required for protein import into the nucleus. Nature *365*, 661–663.

Moreland, R.B., Langevin, G.L., Singer, R.H., Garcea, R.L., and Hereford, L.M. (1987). Amino acid sequences that determine the nuclear localization of yeast histone 2B. Mol. Cell. Biol. *7*, 4048–4057.

Nehrbass, U., Kern, H., Mutvei, A., Horstmann, H., Marshallsay, B., and Hurt, E.C. (1990). NSP1: A yeast nuclear envelope protein localized at the nuclear pores exerts its essential function by its carboxy-terminal domain. Cell *61*, 979–989.

Newmeyer, D.D. (1993). The nuclear pore complex and nucleocytoplasmic transport. Curr. Opin. Cell Biol. *5*, 395–407.

Pante, N., and Aebi, U. (1993). The nuclear pore complex. J. Cell Biol. *122*, 977–984.

Reichelt, R., Holzenburg, A., Buhle, E.L., Jr., Jarnik, M., Engel, A., and Aebi, U. (1990). Correlation between structure and mass distribution of the nuclear pore complex and of distinct pore complex components. J. Cell Biol. *110*, 883–894.

Ren, M., Drivas, G., D'Eustachio, P., and Rush, M.G. (1993). Ran/TC4: a small nuclear GTP-binding protein that regulates DNA synthesis. J. Cell Biol. *120*, 313–323.

Richardson, W.D., Mills, A.D., Dilworth, S.M., Laskey, R.A., and Dingwall, C. (1988). Nuclear protein migration involves two steps: rapid binding at the nuclear envelope followed by slower translocation through nuclear pores. Cell *52*, 655–664.

Riles, L., Dutchik, J.E., Baktha, A., McCauley, B.K., Thayer, E.C., Leckie, M.P., Braden, V.V., Depke, J.E., and Olson, M.V. (1993). Physical maps of the six smallest chromosomes of *Saccharomyces cerevisiae* at a resolution of 2.6 kilobase pairs. Genetics *134*, 81–150.

Ris, H., and Malecki, M. (1993). High-resolution field emission scanning electron microscope imaging of internal cell structures after Epon extraction from sections: a new approach to correlative ultrastructural and immunocytochemical studies. J. Struct. Biol. *111*, 148–157.

Rose, M.D., Winston, F., and Hieter, P. (1989). Methods In Yeast Genetics. Cold Spring Harbor, NY: Cold Spring Harbor Laboratory Press.

Rothstein, R. (1991). Targeting, disruption, replacement, and allele rescue: integrative DNA transformation in yeast. Methods Enzymol. *194*, 281–301.

Rout, M.P., and Blobel, G. (1993). Isolation of the yeast nuclear pore complex. J. Cell Biol. *123*, 771–783.

Rout, M.P., and Wente, S.R. (1994). Pores for thought: nuclear pore complex proteins. Trends Cell Biol. *4*, 357–365.

Schlenstedt, G., Hurt, E., Doye, V., and Silver, P.A. (1993). Reconstitution of nuclear protein transport with semi-intact yeast cells. J. Cell Biol. *123*, 785–798.

Schlenstedt, G., Saavedra, C., Loeb, J.D.J., Cole, C.N., and Silver, P.A. (1995). The GTP-bound form of the yeast Ran/TC4 homologue blocks nuclear protein import and appearance of poly $(A)^+$ RNA in the cytoplasm. Proc. Natl. Acad. Sci. USA *92*, 225–229.

Severs, N.J., Jordan, E.G., and Williamson, D.H. (1976). Nuclear pore absence from areas of close association between nucleus and vacuole in synchronous yeast cultures. J. Ultrastruct. Res. *54*, 374–387.

Sherman, F. (1991). Getting started with yeast. Methods Enzymol. *194*, 3–21.

Sikorski, R.S., and Hieter, P. (1989). A system of shuttle vectors and yeast host strains designed for efficient manipulation of DNA in *Saccharomyces cerevisiae*. Genetics *122*, 19–27.

Silver, P.A. (1991). How proteins enter the nucleus. *Cell* 64, 489–497.

Snow, C.M., Senior, A., and Gerace, L. (1987). Monoclonal antibodies identify a group of nuclear pore complex glycoproteins. J. Cell Biol. *104*, 1143–1156.

Stevens, B.J., and Swift, H. (1966). RNA transport from nucleus to cytoplasm in *Chironomus* salivary glands. J. Cell Biol. *31*, 55–77.

Stewart, M. (1992). Nuclear pore structure and function. Semin. Cell Biol. *3*, 267–277.

Sukegawa, J., and Blobel, G. (1993). A nuclear pore complex protein that contains zinc finger motifs, binds DNA, and faces the nucleoplasm. Cell *72*, 29–38.

Unwin, P.N., and Milligan, R.A. (1982). A large particle associated with the perimeter of the nuclear pore complex. J. Cell Biol. *93*, 63–75.

Wente, S.R., and Blobel, G. (1993). A temperature-sensitive *NUP116* null mutant forms a nuclear envelope seal over the yeast nuclear pore complex thereby blocking nucleocytoplasmic traffic. J. Cell Biol. *123*, 275–284.

Wente, S.R., and Blobel, G. (1994). *NUP145* encodes a novel yeast glycine-leucine-phenylalanine-glycine (GLFG) nucleoporin required for nuclear envelope structure. J. Cell Biol. *125*, 955–969.

Wente, S.R., Rout, M.P., and Blobel, G. (1992). A new family of yeast nuclear pore complex proteins. J. Cell Biol. *119*, 705–723.

Wimmer, C., Doye, V., Grandi, P., Nehrbass, U., and Hurt, E.C. (1992). A new subclass of nucleoporins that functionally interact with nuclear pore protein NSP1. EMBO J. *11*, 5051–5061.

Wozniak, R.W., Blobel, G., and Rout, M.P. (1994). POM152 is an integral protein of the pore membrane domain of the yeast nuclear envelope. J. Cell Biol. *125*, 31–42.

Yano, R., Oakes, M., Yamaghishi, M., Dodd, J.A., and Nomura, M. (1992). Cloning and characterization of *SRP1*, a suppressor of temperature-sensitive RNA polymerase I mutations, in *Saccharomyces cerevisiae*. Mol. Cell. Biol. *12*, 5640–5651.

Yano, R., Oakes, M.L., Tabb, M.M., and Nomura, M. (1994). Yeast Srp1p has homology to armadillo/plakoglobin/β-catenin and participates in apparently multiple nuclear functions including the maintenance of nucleolar structure. Proc. Nat. Acad. Sci. USA *91*, 6880–6884.